Modelling of the inhomogeneous interior of polymer gels

2006 J. Phys.: Condens. Matter 18 3549

(http://iopscience.iop.org/0953-8984/18/15/003)

INSTITUTE OF PHYSICS PUBLISHING JOURNAL OF PHYSICS: CONDENSED MATTER

J. Phys.: Condens. Matter **18** (2006) 3549–3562 doi:10.1088/0953-8984/18/15/003

Modelling of the inhomogeneous interior of polymer gels

Chwen-Yang Shew[1] **and Takafumi Iwaki**[2]

[1] Center for Engineered Polymeric Materials (CEPM), Department of Chemistry and Graduate Center, City University of New York, College of Staten Island, 2800 Victory Boulevard, NY 10314, USA
[2] Okayama Institute for Quantum Physics, 1-9-1 Kyoyama, Okayama 700-0015, Japan

E-mail: shew@mail.csi.cuny.edu

Received 10 February 2006
Published 30 March 2006
Online at stacks.iop.org/JPhysCM/18/3549

Abstract

A simple model has been investigated to elucidate the mean squared displacement (MSD) of probe molecules in cross-linked polymer gels. In the model, we assume that numerous cavities distribute in the inhomogeneous interior of a gel, and probe molecules are confined within these cavities. The individual probe molecules trapped in a gel are treated as Brownian particles confined to a spherical harmonic potential. The harmonic potential is chosen to model the effective potential experienced by the probe particle in the cavity of a gel. Each field strength is corresponding to the characteristic of one type of effective cavity. Since the statistical distribution of different effective cavity sizes is unknown, several distribution functions are examined. Meanwhile, the calculated averaged MSDs are compared to the experimental data by Nisato *et al* (2000 *Phys. Rev.* E **61** 2879). We find that the theoretical results of the MSD are sensitive to the shape of the distribution function. For low cross-linked gels, the best fit is obtained when the interior cavities of a gel follow a bimodal distribution. Such a result may be attributed to the presence of at least two distinct classes of cavity in gels. For high cross-linked gels, the cavities in the gel can be depicted by a single-modal uniform distribution function, suggesting that the range of cavity sizes becomes smaller. These results manifest the voids inside a gel, and the shape of distribution functions may provide the insight into the inhomogeneous interior of a gel.

1. Introduction

Polymer gels are one of the most studied materials because of their unique properties and enormous industrial applications [1]. Recently, Nisato and co-workers devised a tracer particle method to explore the interior of a cross-linked gel [2]. In their experiment, charged colloidal particles, as probes, were introduced into like-charged polyelectrolyte gels. A dynamical

light scattering experiment was conducted to characterize the time-dependent mean squared displacement (MSD) of the probes in a gel. Such a design prevents the physical adsorption of colloidal particles onto a cross-linked gel, and enables the colloidal particles to probe the interior of a gel.

In the experiment by Nisato and co-workers, they found that the probe molecules are essentially confined in gels, and the dynamics of probe molecules is quite sensitive to the cross-linking ratio of the gel. They found that the MSD of probe molecules increases first and reaches a plateau after a long enough time. The plateau indicates that probe molecules are trapped locally in a gel, possibly within some cavities. As the cross-linking ratio is increased, the MSD approaches the plateau at a shorter time, and the magnitude of the plateau becomes smaller. These results suggest that at a higher cross-linking ratio, the confinement inside a gel becomes even more significant.

In addition to the above-mentioned dynamical scattering experiment, Yamane and co-workers have carried out a different experiment to measure the dynamics of small amino acids, as probe molecules, in a cross-linked polymer gel by using the NMR method [3]. They found that the measured diffusion coefficients are sensitive to the timescale. For short diffusion time, the diffusion coefficient consists of two major components due to non-uniform network sizes (i.e. cavity sizes). Note that such observation is quite similar to the finding of the two types of cavity size present in silica gels and aluminosilicate gels [4, 5]. For long diffusion time, the diffusion coefficient displays only one component. They argued that the single diffusion coefficient is due to averaging over all network sizes. Furthermore, the diffusion lengths obtained from the NMR data are found at the lengthscale of μm between the mesh size (network size in nm) and the size of a swollen gel (a few hundreds of μm). Their results provide evidence for the inhomogeneous nature of a gel, and the measured diffusion lengths may link with the size of cavities (or voids) in gels.

To better understand the inhomogeneous interior of gels, Ngai and co-workers have employed the dynamical light scattering method for photo-cross-linkable gels [6, 7]. After a photocycloaddition reaction is induced, the semidilute polymer solution is transformed into polymer gels. By increasing the cross-linking density of gels, the scattering intensity increases. Such a result contradicts the traditional picture that the gel becomes more uniform at greater cross-linking densities, and the scattering intensity of a perfect 'uniform' gel should totally diminish due to cancellation of signals isotropically. Since the mesh size (compared to the semidilute solution) is not changed significantly during gel formation, an increase of the scattering intensity is attributed to the formation of large voids in gels, with size greater than the mesh size but smaller than the total dimension of a gel. This result is consistent with the NMR experiment by Yamane *et al* [3].

As pointed out by Wu [8], the origin of the inhomogeneous gel interior arises from the fact that the cross-linking reaction is a diffusion control process during gel formation. The random nature of the cross-linking reaction results in an inhomogeneous monomer density distribution, with various cavity sizes. As a result, the spatial distribution of cavities can be quite random, and the scattering signals are enhanced. These findings may change the way to understand polymer gels. The mesh size, the average length between neighboring cross-linked sites, widely used to characterize the properties of gels, is only useful at the local lengthscale, but it may not be sufficient to detail the interior structure of gels.

In this work, we investigate a simple model to elucidate the dynamics of a probe molecule in cross-linked gels. This model is an extension of our previous work for macromolecules confined to harmonic potentials [9]. Here the harmonic potential is chosen to depict the effective interaction potential experienced by the probe particle in a cavity of cross-linked gels. Since the gel contains water and dangling branches, we assume that the colloidal particles

undergo Brownian motion. Namely, the system is simplified to a Brownian particle in a harmonic potential. Each force constant (or field strength) of harmonic potential represents one type of cavity. Since the size of cavities in a gel may vary widely, we examine several possible distribution functions, with the aim of finding an appropriate distribution to model different effective cavity (or void) sizes.

2. Model

2.1. Brownian particles in harmonic potentials

The starting point of this work is to treat the probe molecule trapped in the cavity of a gel as a Brownian particle confined to a spherical harmonic potential, a classical model in literature [9, 10]. The Brownian motion is exploited to model the friction and collisions arising from solvent molecules and side branches in gels. The motion of a probe molecule is therefore given by

$$\zeta \frac{\partial R}{\partial t}(t) = -kR(t) + f(t) \tag{1}$$

where $R(t)$ is the instantaneous location of the probe; k is the strength of the harmonic potential; ζ is the frictional coefficient of the probe molecule; $f(t)$ are the random forces satisfying $\langle f_\alpha(t) f_\beta(t')\rangle = 2\delta_{\alpha\beta}\zeta k_B T \delta(t - t')$, where $\alpha, \beta = x, y, z$. Since the mass of a latex colloid is large, the inertial term is neglected [9, 10]. With some algebra, the mean squared displacement (MSD) can be formulated as follows.

$$\langle (R(t) - R(0))^2 \rangle = \frac{6k_B T}{k}\left[1 - \exp\left(-\frac{kt}{\zeta}\right)\right]. \tag{2}$$

At the short time limit ($t \to 0$),

$$\langle (R(t) - R(0))^2 \rangle = \frac{6k_B T}{\zeta} t, \tag{3}$$

suggesting that the MSD should be independent of external fields. For $t \gg 1$, $\langle (R(t) - R(0))^2 \rangle = 6k_B T/k$. Actually, equation (2) is equivalent to the model in which a mean cavity is utilized to represent all possible cavities in a gel [11].

In the above model, the harmonic potential is chosen to mimic the effective potential experienced by the probe molecule confined to a cavity. First, in the experimental design, the like-charged colloid particles are introduced to avoid their physical adsorption on the polymer gel. The harmonic potential used in this work is repulsive, and is a simple model to depict the repulsion between a colloid particle and the like-charged gel. Since the gel and colloidal particles investigated in the experiment are both ionic, some water molecules may be tightly bound to the charged groups in the gel. These adsorbed water molecules can be viewed as small springs, and the force constant of the harmonic potential becomes the effective spring constant of these smaller springs. Moreover, the harmonic potential is a simplified representation for the local elasticity inside a gel. Actually, the harmonic potential accounts for various fundamental interactions between the probe particle and the polymer gel.

2.2. Size distribution of cavities in gels

Due to the inhomogeneous nature of gelling materials, different types of (effective) cavity may randomly distribute in a gel. Note that the cavity size in this work is referred to the effective dimension in a cavity within which the probe molecule is allowed to move. The colloidal particles chosen in the experiment by Nisato and co-workers probe those cavities close to or

greater than the size of the probe molecule. In our model, each type of cavity is characterized by a harmonic potential of strength k. By assuming that the cavities in gels are uncorrelated, the measured mean squared displacement is obtained from averaging over the distribution function of different cavity sizes $P(k)$, given by

$$\langle (R(t) - R(0))^2 \rangle_e = \int_{k_{min}}^{k_{max}} dk\, P(k) \langle (R(t) - R(0))^2 \rangle. \tag{4}$$

This equation incorporates multiple cavities, which is beyond the empirical correction for the disorder environment of a gel [2].

Since the probability distribution of different types of cavity, $P(k)$, is unknown, several distribution functions are considered, including the following.

(A) *Uniform distribution*

$$P(k) = H(k - a)H(b - k)/(b - a) \tag{5}$$

where $H(k - x)$ is the Heaviside step function; a and b equal k_{min} and k_{max}, respectively (the range of k). In the calculations, the variables a and b are two adjustable parameters. In addition to the uniform distribution, the following three functions ((B)–(D)) are chosen to test the shape effect of distribution functions.

(B) *Gaussian distribution*

$$P(k) = \frac{\exp[-b^2(k - a)^2]}{\int_{k_{min}}^{k_{max}} dk \exp[-b^2(k - a)^2]} \tag{6}$$

where a and b are adjustable parameters; k varies from $k_{min} = 0$ to $k_{max} = \infty$. The statistical weight decays when k shifts away from a. Basically, the cavities of larger k are screened out more in this distribution function, particularly for smaller a.

(C) *Inverse uniform distribution*

$$P(k) = \frac{1}{k^2} \frac{H(k - 1/a)H(1/b - k)ab}{(a - b)}. \tag{7}$$

The inverse uniform distribution is used to transform the variable k in the uniform distribution function into $1/k$.

(D) *Inverse Gaussian distribution*

$$P(k) = \frac{\exp[-b^2(\frac{1}{k} - a)^2]}{\int_{k_{min}}^{k_{max}} dk \exp[-b^2(\frac{1}{k} - a)^2]} \tag{8}$$

where a and b are adjustable parameters; k varies from $k_{min} = 0$ to $k_{max} = \infty$. As in inverse uniform distribution, the inverse Gaussian distribution transforms k used in the Gaussian function into $1/k$.

(E) *Exponential decay function*

In contrast to the above distribution functions, we also consider an adjustable exponential decay function.

$$P(k) = \frac{m \exp(-mk)}{\exp(-mk_{min}) - \exp(-mk_{max})} \tag{9}$$

where m is an adjustable parameter relevant to the width of the exponential decay function. The exponential decay function is selected to reduce the statistical weight of cavities of larger k, as opposed to the distribution functions in equations (7), (8).

(F) *Bimodal distribution function*

The distribution functions (A)–(E) consist of only one maximum (single modal) in the range of our interest. Actually, several experimental works have shown that the gel interior

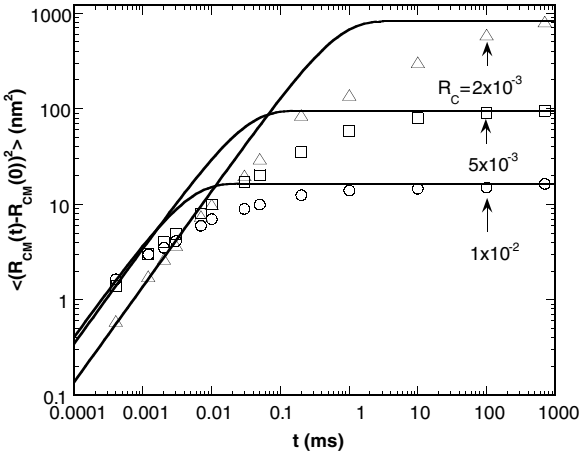

Figure 1. Plot of the measured and the calculated MSD based on equation (2), denoted by symbols and lines, respectively, for different cross-linking ratios R_c, as marked; the experimental data are extracted from [2].

consists of two types of cavity [3–5]. Likewise, the two types of cavity may display a bimodal distribution due to size fluctuation. To test the possibility of the formation of bimodal distribution in gels, a simple distribution function is investigated. In the model, the two peaks of a bimodal distribution function are considered to be two uniform distribution functions with the same width: one ranges from $k = k_0$ to k_1 and the other ranges from $k = k_2$ to $k_2 + k_1 - k_0$. Moreover, a probability parameter, p, is incorporated into the distribution function to adjust the statistical weight of the two peaks, which reads

$$P(k) = \frac{1}{(k_1 - k_0)}\{(1-p)H(k-k_0)H(k_1-k) + (p)H(k-k_2)H[(k_2+k_1-k_0)-k]\}. \tag{10}$$

In spite of its simplicity, this distribution function is useful for dividing the possible cavities into two distinct groups: smaller and greater k.

3. Results and discussion

3.1. Single mean cavity

We first study the case in which all types of cavity in the gel can be represented by one single cavity, i.e., a mean effective cavity. In the calculations, we apply equation (3) to fit the measured MSD at the shortest time ($t = 4 \times 10^{-4}$ ms) from the experiment by Nisato and co-workers [2]. The procedure is to determine the frictional coefficient ζ for each cross-linking ratio R_c, in the hope that the timescale at this point is short enough to approach the short time limit of MSD. With this ζ, equation (2) consists of only one adjustable parameter k (i.e., mean effective cavity), and is applied to fit the measured MSD at the longest time in the experiment (about 800 ms) for a given cross-linking ratio R_c. The calculated ζ and the fitted k for different R_c are summarized in table 1. Figure 1 compares the measured and the calculated MSD based on equation (2), denoted by symbols and lines, respectively, for different R_c, as marked. Equation (2) predicts a plateau, consistent with the experimental observation. However, the model deviates from the experiment appreciably in the intermediate timescale before reaching the plateau [2]. The deviation may be attributed to the fact that gels consist of multiple types of cavity, other than one single type.

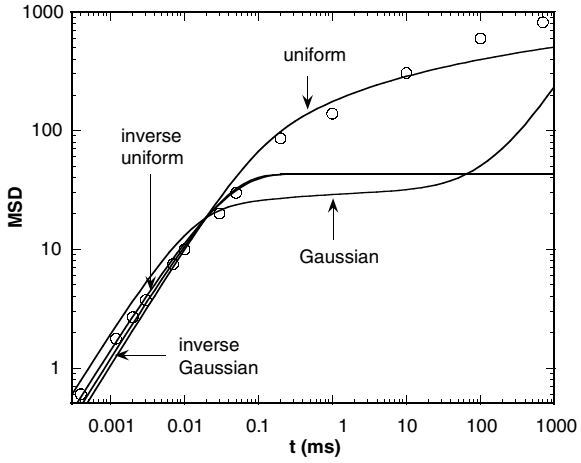

Figure 2. Plot of the best fit of the average MSD predicted by different distribution functions from equation (5) to (8), and experimental data, denoted by symbols, for the cross-linking ratio $R_c = 5 \times 10^{-3}$.

Table 1. Fitted parameters from the model based on equation (2) for different cross-linking ratios R_c.

R_c	ζ/k_BT (s nm^{-2})	k/k_BT (nm^{-2})
2×10^{-3}	4.00×10^{-3}	0.003 66
5×10^{-3}	1.72×10^{-3}	0.031 7
1×10^{-2}	1.46×10^{-3}	0.183

Table 2. Fitted parameters from the trial distribution functions for cross-linking ratio $R_c = 5 \times 10^{-3}$.

Distribution function	a/k_BT (nm^{-2})	b/k_BT (nm^{-2})	ζ/k_BT
Uniform	1.0×10^{-7}	0.430	1.72×10^{-3}
Gaussian	0.147	11.7	3.04×10^{-3}
Inverse uniform	5.22×10^{-20}	1.25×10^{-4}	4.18×10^{-3}
Inverse Gaussian	14.2	2.5×10^{20}	5.03×10^{-3}

3.2. Comparison of size distribution functions

To incorporate multiple cavities into the model, an appropriate distribution function is needed to account for the statistical weight of different cavity sizes in a gel. Since the best choice of distribution function is unknown, it would be instructive to examine a few possible functions. Here, we test a series of distribution functions summarized in (equations (5)–(8)). Equation (5) treats various cavities as a uniform distribution function, whereas equation (6) is a Gaussian function with a maximum at finite k. The other two distribution functions in equations (7) and (8) tend to have a larger statistical weight for greater k.

For a given distribution function, equation (4) is then applied to compute the average MSD (by averaging over the distribution function). In addition to the adjustable parameters in the distribution functions (equations (5)–(8)), the frictional coefficient ζ is treated as a fitting parameter as well (only in this section). Figure 2 compares the best fit of the average MSD predicted by using different distribution functions, as marked, with experimental data, denoted by symbols, for the cross-linking ratio $R_c = 5 \times 10^{-3}$. The fitting parameters are summarized in table 2. We find that the uniform distribution function (equation (5)) results in the best fit compared to the experimental data. In contrast to uniform distribution function, the Gaussian

distribution fails to fit the data because the statistical weight decreases continuously towards smaller and larger k from the central peak of the distribution function. Meanwhile, the results of both inverse uniform and inverse Gaussian distribution functions are quite similar. Both show poor agreement compared to the experimental data, and their plateau values are much smaller than the experimental results. Actually, both distribution functions overestimate the contribution arising from large k. These results suggest that to better fit the experimental data, the shape of the distribution function is crucial, and the distribution function is required to cover a wide range of k, including k close to zero.

3.3. Uniform distribution function

The above comparison for various distribution functions suggests that the uniform distribution function in equation (5) is a reasonable choice to quantify the experimental data. In this section, we focus on the calculations based on this distribution function, equation (5). This model assumes that the strength of harmonic potential k is evenly distributed in the range between $k_{\min}$ and $k_{\max}$ (lower bound and upper bound of k). The mean MSD, $\langle (R(t) - R(0))^2 \rangle_e$, is calculated by averaging over the range of field strengths, given by

$$\begin{aligned}\langle (R(t) - R(0))^2 \rangle_e &= \frac{6k_BT}{(k_{\max} - k_{\min})} \int_{k_{\min}}^{k_{\max}} dk \frac{1}{k}\left[1 - \exp\left(-\frac{kt}{\zeta}\right)\right] \\ &= \frac{6k_BT}{(k_{\max} - k_{\min})}[\ln(k_{\max}/k_{\min}) + E_1(k_{\max}t/\zeta) - E_1(k_{\min}t/\zeta)] \end{aligned} \tag{11}$$

where E_1 is the exponential integral. In the above equation, the two asymptotic expressions for long and short timescales are given as follows. For $t \gg 1$, $\langle (R(t) - R(0))^2 \rangle_e = 6k_BT \ln(k_{\max}/k_{\min})/(k_{\max} - k_{\min})$, and for $t \ll 1$, $\langle (R(t) - R(0))^2 \rangle_e$ is reduced to equation (3). To this end, the investigated model involves three adjustable variables: ζ, $k_{\min}$ and $k_{\max}$. Among these variables, ζ can be determined from the short-time dynamics because MSD becomes independent of field strength as $t \to 0$, as shown in equation (3). Note that the fitted frictional coefficients in table 2 are quite close to those in table 1. In the rest of this paper, the frictional coefficients are fixed and are selected from table 1. With the fixed frictional coefficient, the adjustable parameters are now reduced to the range of field strength k, i.e., $k_{\min}$ and $k_{\max}$. This modified model, with multiple cavities incorporated, undertakes the analysis beyond the empirical correction for the disorder environment of a gel, as seen in the literature [2].

The agreement between theory and experiment is improved by using equation (11). Figure 3 is the same as figure 1 except that equation (11) is used for the theoretical calculation. Table 3 summarizes the fitted $k_{\min}$ and $k_{\max}$. As in figure 1, the MSD first increases and then reaches a plateau when time is increased, indicating that the particle cannot drift away from a confined boundary (i.e., a cavity). The plateau value is close to $6k_BT \ln(k_{\max}/k_{\min})/(k_{\max} - k_{\min})$, the long time limit of equation (11). For larger R_c, the MSD reaches plateau at a shorter time, and the value of plateau becomes smaller. In table 1, we find that as R_c is increased, the fitted ζ decreases. Furthermore, in table 2, $k_{\max}$ and $k_{\min}$ shift toward larger values, and the range of k becomes narrower for lager R_c. As a matter of fact, the fitted $k_{\min}$ and $k_{\max}$ enable us to evaluate the range of effective cavity sizes. The corresponding MSD for $k_{\min}$ and $k_{\max}$ allow us to estimate the range of effective cavity sizes, by summing up the minimum (or maximum) dimension estimated from MSD and the physical size of probe particles (around 85 nm). The estimations are summarized in table 3, and the findings show that for larger R_c, the range of effective cavity sizes becomes narrower.

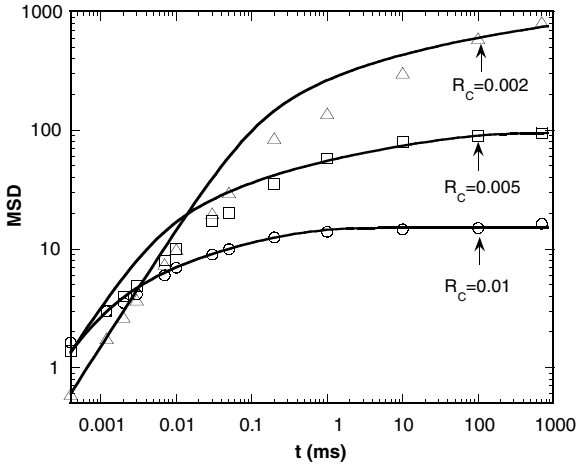

Figure 3. Same as figure 1 except that equation (11) is chosen for the theoretical calculation; the experimental data are extracted from [2].

Table 3. Fitted parameters from the model based on equation (11) for different cross-linking ratios R_c.

R_c	k_{min}/k_BT (nm^{-2})	k_{max}/k_BT (nm^{-2})	Range of cavity sizes (nm)
2×10^{-3}	≈ 0	0.0820	$\sim$90–($\gg$90)
5×10^{-3}	8.48×10^{-6}	0.718	90–930
1×10^{-2}	1.27×10^{-3}	3.12	90–150

The above results can be further understood as follows. For the greater cross-linking ratio R_c, more polymer chains in the gel are linked chemically, and the amounts of dangling branches decrease. When the number of links is increased, the size of cavities decreases, and the rigidity of the interior cavities of a gel increases. The shift of the plateau of the MSD towards a shorter timescale and a smaller value in figures 1 and 2 for the greater R_c arises from the more pronounced confinement effect within a smaller cavity. Moreover, as pointed out by Nisato *et al* [2], dangling branches may have a substantial contribution to the frictional forces experienced by the probe molecule, and a decrease of dangling branches would reduce the frictional coefficient.

3.4. Exponential decay functions

To further test the size distribution of cavities, we carry out the calculations by using the exponential decay function in equation (9). Such a function approaches the uniform distribution function when m becomes very small, and enables us to attenuate the statistical weight of larger k (or smaller cavities) in the distribution function as the parameter m is increased. This distribution function emphasizes on smaller k, as opposed to the inverse uniform and inverse Gaussian functions in equations (7) and (8) with a greater statistical weight for larger k.

Figure 4 plots the best fit of the MSD for $R_c = 0.002$, obtained from the exponential decay function with $m = 14$ and 0.01. To obtain the best fit, k_{min} needs to be set to *zero* regardless of our choice of m. For smaller m, such as $m = 0.01$, the best fit of the MSD calculated from the exponential decay function and from the uniform distribution function is essentially the same. As m is increased to 14, the fitting is not very different from that for $m = 0.01$. However, it is noticeable that for larger m ($m > 14$), the exponential decay function fails to fit the experimental data. The calculated MSD with larger m at the longest experimental timescale

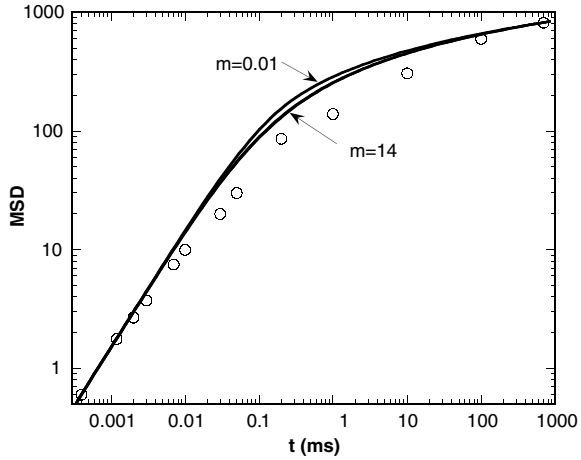

Figure 4. Plot of the best fit of the MSD of $R_c = 0.002$ using the exponential decay function for $m = 14$ and 0.01.

is much greater than that of the experimental measurement. The poor agreement for m greater than 14 is because large enough k in the distribution function are screened out. This result also suggests that probe molecules reside in both smaller (with greater k) and larger (with smaller k) cavities of a gel.

3.5. Bimodal against single modal distribution

Despite the fact that the uniform distribution improves the fitting of experimental data, a small discrepancy remains between theory and experiment, and the discrepancy is enhanced as the cross-linking ratio R_c is decreased in figure 3. The discrepancy may imply that a different type of distribution function is needed. To improve the small deviation in fitting, we resort to equation (10), consisting of two peaks in the bimodal distribution function, and each peak is composed of a uniform distribution function. The average MSD takes the following form:

$$\begin{aligned}\langle (R(t) - R(0))^2 \rangle_e &= 6k_B T \left\{ \frac{1-p}{k_1 - k_0} \left[\ln\left(\frac{k_1}{k_0}\right) + E_1\left(\frac{k_1 t}{\zeta}\right) \right.\right. \\ &\quad \left. - E_1\left(\frac{k_0 t}{\zeta}\right) \right] + \frac{p}{k_1 - k_0} \left[\ln\left(\frac{k_2 + k_1 - k_0}{k_2}\right) \right. \\ &\quad \left.\left. + E_1\left(\frac{(k_2 + k_1 - k_0)t}{\zeta}\right) - E_1\left(\frac{k_2 t}{\zeta}\right) \right] \right\}. \end{aligned} \tag{12}$$

In the calculations, we choose $k_0 \to 0$ (because the best fit is obtained by letting $k_0 \to 0$ for $R_c = 0.002$ from our test). Note that the fitting requires two parameters: k_1 and k_2. In figure 5, we plot the best fit of the MSD for $R_c = 0.002$, and for $p = 0.5$, 0.67, 0.8 and 0.9, as marked, by using equation (12). For comparison, the best fit resulting from the uniform distribution is also plotted as a dotted–dash line. The fitted parameters are summarized in table 4. Generally, the agreement between the theory and experiment is enhanced as p is increased. Actually, in the experiment, the data of $R_c = 0.002$ were determined by using two different experimental methods, due to two distinct timescales. The experimental data are not available in the region roughly around $t = 0.1$ ms. As a result, an accurate fitting is impeded. From inspection, we may argue that $p = 0.8$ yields the best fit compared to the experiment even though its error is slightly larger than that of $p = 0.9$ in the calculations. This argument is based on the fact that the theoretical curve of $p = 0.8$ evenly pass through all the data points, whereas a significant

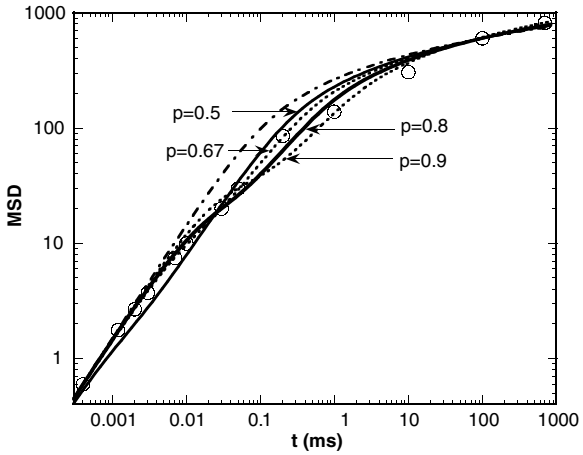

Figure 5. Comparison of the calculated MSD for $p = 0.5$, 0.67, 0.7 and 0.9 by using a bimodal distribution, as marked, and uniform distribution (dotted–dash line) with experimental data (symbols) for $R_c = 0.002$.

Table 4. Fitted parameters from the model based on equation (11) for cross-linking ratio $R_c = 0.002$ and $k_0 = 0$.

p	k_1/k_BT (nm^{-2})	k_2/k_BT (nm^{-2})
0.5	3.71×10^{-2}	5.70
0.67	2.34×10^{-2}	0.689
0.8	1.30×10^{-2}	0.401
0.9	5.63×10^{-3}	0.221

deviation is observed in the curve of $p = 0.9$ at around $t = 0.2$ ms. Since k_1 is quite small and is close to zero, one may speculate that some of probe molecules remain outside the gel or stay in large enough cavities of which the environments are similar to the bulk solution (outside the gel).

Moreover, figure 5 shows that the single modal uniform distribution function tends to overestimate the MSD perceptibly, at an intermediate timescale, about $t = 0.01$–10 ms. In contrast, the bimodal distribution function can be utilized to adjust the calculated curve in this region. Compared to the result fitted with the uniform distribution function (dotted–dash line), the bimodal distribution is in better agreement with experiment.

Although the width of the two peaks is chosen to be the same in the calculations, the average MSD in equation (12), indeed, can be generalized as follows.

$$\begin{aligned}\langle (R(t) - R(0))^2 \rangle_e &= 6k_BT \left\{ \frac{w_A(1-p)}{w_A(k_1-k_0)} \left[\ln\left(\frac{w_A k_1}{w_A k_0}\right) + E_1\left(\frac{w_A k_1 t}{w_A \zeta}\right) \right.\right. \\ &\quad \left. - E_1\left(\frac{w_A k_0 t}{w_A \zeta}\right) \right] + \frac{w_B p}{w_B(k_1-k_0)} \left[\ln\left(\frac{w_B(k_2+k_1-k_0)}{w_B k_2}\right) \right. \\ &\quad \left.\left. + E_1\left(\frac{w_B(k_2+k_1-k_0)t}{w_B \zeta}\right) - E_1\left(\frac{w_B k_2 t}{w_B \zeta}\right) \right] \right\} \qquad (13)\end{aligned}$$

where w_A and w_B are scaling factors to adjust the widths of the two peaks in the bimodal distribution, which are under the constraint $w_A(1-p) + w_B p = 1$. In other words,

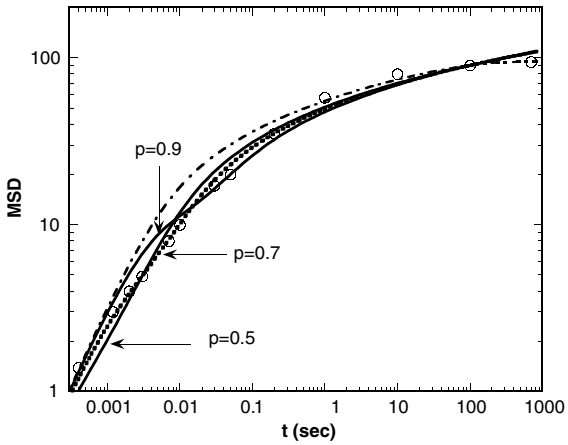

Figure 6. Comparison of the calculated MSD for $p = 0.5$, 0.7 and 0.9 by using a bimodal distribution, as marked, and a uniform distribution (dotted–dash line) with experimental data (symbols) for $R_c = 0.005$.

Table 5. Fitted parameters from the model based on equation (11) for cross-linking ratio $R_c = 0.005$ and $k_0 = 0$.

p	k_1/k_BT (nm^{-2})	k_2/k_BT (nm^{-2})
0.5	0.351	7.63
0.7	0.204	1.91
0.9	6.47×10^{-2}	0.621

equation (10) can be viewed as a model consisting of two classes of cavity, corresponding to the two peaks in the bimodal distribution. These two classes of cavity have distinct environments, including different frictional coefficients ($w_A\zeta$ and $w_B\zeta$) and different peak widths ($w_A(k_1 - k_0)$ and $w_B(k_1 - k_0)$). Namely, equation (13) suggests that multiple distinct cavities are present in the inhomogeneous interior of a gel. On the other hand, this equation casts some uncertainty regarding how to determine the true distribution function because the parameters in equation (13) yield multiple solutions from the limited experimental data.

In addition to the fitting for $R_c = 0.002$, equation (12) is further extended to fit the MSD data for $R_c = 0.005$. Figure 6 compares the calculated MSD for $p = 0.5$, 0.7 and 0.9 by using a bimodal distribution, as marked, and a single modal uniform distribution (dotted–dash line) with experimental data (symbols). The fitted parameters are summarized in table 5. We find that the single modal uniform distribution function displays a greater discrepancy for a timescale roughly less than 1 ms. However, the agreement between theory and experiment is enhanced when a bimodal distribution is applied. Among different p, the best fit occurs at around $p = 0.7$. Also, tables 4 and 5 imply that as the cross-linking ratio R_c is increased, the size range of each class of cavity tends to decrease (k_1 and k_2 in a similar order of magnitude for greater R_c), and the number of cavities with greater k increases.

When R_c is increased to 0.01, the gel undergoes even more cross-linking, and the distribution of cavity sizes exhibits different behaviour. Figure 7 compares the calculated MSD for $p = 0.5$, 0.67 and 0.8 obtained from the bimodal distribution, as marked, and from the single modal uniform distribution (dotted–dash line) with the experimental data (symbols). Like figures 5 and 6, we first choose $k_0 = 0$ in the bimodal distribution function. When the bimodal distribution is applied, the optimal fitting leads to the result of $k_1 = k_2$ (as in table 6),

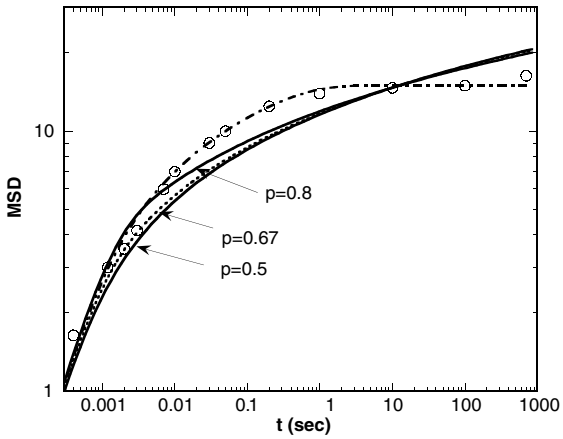

Figure 7. Comparison of the calculated MSD for $p = 0.5$, 0.67 and 0.8 by using a bimodal distribution, as marked, and a uniform distribution (dotted–dash line) with experimental data (symbols) for $R_c = 0.01$.

Table 6. Fitted parameters from the model based on equation (11) for cross-linking ratio $R_c = 0.01$ and $k_0 = 0$.

p	k_1/k_BT (nm^{-2})	k_2/k_BT (nm^{-2})
0.5	2.22	2.22
0.67	1.53	1.53
0.8	0.994	0.994

and such a result is independent of our choice of p. Nevertheless, the discrepancy remains large between theory and experiment as long as a bimodal distribution function is utilized. Actually, the best fit to the experimental data is obtained by using a uniform distribution function along with a finite k_{min} as discussed in section 3.3. These results indicate that for larger R_c, the cavities of smaller k (larger cavities) diminish, and the two distinct classes of cavity may merge into one class. Together with the size range estimated in table 1, we may argue that for large R_c, the gel undergoes more cross-linking. As a result, the cavities inside a gel are smaller, and their sizes become more uniform. This result is not inconsistent with the conclusion drawn by Ngai and co-workers because the random distribution of these smaller cavities may enhance the scattering signal of gels as long as their spatial distribution is non-uniform [2].

Equations (11) and (12) represent the average MSD over the single modal and bimodal distribution, respectively. The curves shown in figures 5, 6 are calculated by using two parameters. Without changing the number of fitting parameters, we find that the best fit for different R_c is governed by the form of distribution function. In other words, the size distribution of cavities is an important factor to elucidate the inhomogeneous interior of gels. As for the shape of the bimodal distribution, a separate study has been conducted to examine a different bimodal distribution function, and the results are summarized in the appendix.

The bimodal distribution may have a physical implication analogous to two coexistent physical states. For smaller cross-linking ratios (e.g., $R_c = 0.002$ and 0.005), the gel interior is composed of two physical states (smaller and larger k). However, for larger cross-linking ratios (e.g., $R_c = 0.01$), the single modal distribution indicates that the gel interior makes a transition to a single physical state (composed of larger k). In addition to the argument based on a thermodynamic phase transition, the single modal size distribution can be understood in

a different way, i.e., the probe molecules chosen in the experiment reside only in the cavities equal to or greater than the probe size. Namely, those cavities smaller than the probe molecules are not sampled. In our view, these speculations can be further tested experimentally. In the former case, the gels may change their physical characteristics more significantly under phase transition. In the latter case, the smaller cavities of greater cross-linking ratios may be detected through smaller probe molecules.

4. Conclusions

We have investigated a simple model to elucidate the dynamics of probe molecules in cross-linked polymer gels. In these models, we assume that probe molecules are confined to the cavities within the gel as single Brownian particles subjected to a harmonic potential (with strength k). The harmonic potential is chosen to model the effective potential experienced by a probe molecule in a gel. To obtain the best fit, we need to select an appropriate distribution function to account for the effective size of all types of cavity within which probe molecules are confined. Also, an additional assumption in these calculations is that the cavities are uncorrelated in the gel. Hence, the mean squared displacement (MSD) is calculated by averaging over the distribution of all types of cavity. We first find that the calculated MSDs are sensitive to the shape of the distribution function. Distribution functions consisting of a range of cavities, including smaller (larger k) and larger (smaller k) cavities, are the most appropriate choices. To better understand the experimental data, we find that the distribution function for low cross-linked and high cross-linked gels should be different. For low cross-linked gels, a bimodal distribution function is required, indicating that at least two classes of cavity are present in the gel. Such a result is consistent with the experimental observation for polymer gels and silica-containing gels. For high cross-linked gel, the single-modal uniform distribution function is sufficient to fit the experimental data. The caveat is that the distribution function should range between two finite values of k, without $k = 0$ involved. Namely, the probe molecules reside in a certain range of cavities. Furthermore, it is noticeable that for the gels of larger cross-linking ratios, the cavity sizes become smaller and more uniform. The transformation between single modal (one state) and bimodal distribution (two states) for different cross-linking ratios may have an implication of phase transition. An alternative explanation is that the probe molecule chosen in the experiment may be too large to explore the smaller cavities for the gels of higher cross-linking ratios. The correlation between cavities is not attainable from this work. Nevertheless, a further experiment can be attempted by monitoring the correlation function between probe molecules.

Acknowledgments

We are grateful for partial support for this work from the City University of New York PSC-CUNY grant No 67666-00-36, NSF Garcia MRSEC at Stony Brook University, NY STAR grant for the Center of Engineered Polymeric Materials at CSI, and the Institute of Macromolecular Assemblies at CSI. CYS thanks Professors S K Kumar and A Yethiraj for stimulating discussions.

Appendix. An alternative function for bimodal distribution

The fitting reported in this work is sensitive to the shape of the distribution function. We have tested an alternative to model the bimodal distribution, which is given by

$$P(k) = \frac{1 + \cos\left(2\pi \frac{k}{k_{\max}} + \phi\right)}{(k_{\max} - k_{\min}) + \frac{k_{\max}}{2\pi}\left[\sin(\phi) - \sin\left(\frac{2\pi k_{\min}}{k_{\max}} + \phi\right)\right]} \tag{A.1}$$

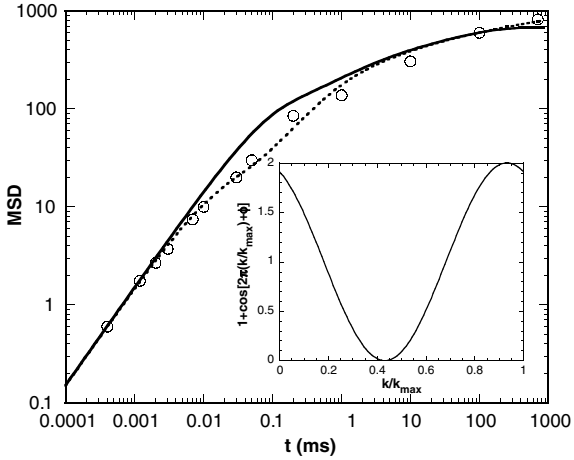

Figure A.1. Comparison of the best fit obtained from equations (10), denoted by the dotted line, and (A.1), denoted by the solid line; the inset displays the fitted distribution function multiplied by the normalization constant.

where ϕ is an adjustable parameter to vary the phase of the cosine function. By shifting ϕ, the position and the statistical weight of the two peaks of the bimodal function can be changed. In the calculations, we first let $k_{\min} = 0$, and select two fitting parameters: $k_{\max}$ and ϕ, as in equation (10). In figure A.1, we compare the best fit obtained from equations (10), denoted by the dotted line, and (A.1), denoted by the solid line; the inset displays the distribution function multiplied by the normalization constant. The best fit is obtained when $k_{\max} = 0.0796$ and $\phi = 0.429$. The distribution show the bimodal feature, with one maximum near 0 and the other near 0.9π. We find that the cosine function lacks the flexibility to adjust the calculated MSD near the time range $t = 0.01$–1 ms. Hence, the agreement with the experimental data for equation (A.1) is not as good as equation (10) based on the bimodal uniform distribution function. Nevertheless, this calculation shows the influence of the shape of the distribution function on the theoretical fitting.

References

[1] Siegel R A 2004 *Fundamentals and Applications of Polymer Gels* (New York: Wiley–VCH)
[2] Nisato G, Hebraud P, Munch J-P and Candau S J 2000 *Phys. Rev.* E **61** 2879
[3] Yamane Y, Matsui M, Kimura H, Kuroki S and Ando I 2003 *Macromolecules* **36** 5655
[4] Rao K S and Das B 1970 *J. Colloid Interface Sci.* **32** 24
[5] Ivanova I I, Aiello R, Nagy J B, Crea F, Derouane E G, Dumont N, Nastro A, Subotic B and Testa F 1994 *Micropor. Mater.* **3** 245
[6] Ngai T and Wu C 2003 *Macromolecules* **36** 848
[7] Ngai T, Wu C and Chen Y 2004 *J. Phys. Chem.* B **108** 5532
[8] Wu C 2005 personal communication (Chinese Hong Kong University)
[9] Wenczel R and Shew C-Y 2002 *J. Chem. Phys.* **116** 9537
[10] Doi M and Edwards S F 1986 *The Theory of Polymer Dynamics* (Oxford: Oxford University Press)
[11] Pusey P N and Van Megen W 1989 *Physica* A **157** 705